

Entanglement and Bell inequalities violation in $H \rightarrow ZZ$ with anomalous coupling

Alexander Bernal*

*Instituto de Física Teórica, IFT-UAM/CSIC,
Universidad Autónoma de Madrid,
Cantoblanco, 28049 Madrid, Spain*

Paweł Caban[†] and Jakub Rembieliński[‡]

*Department of Theoretical Physics, University of Łódź
Pomorska 149/153, PL-90-236 Łódź, Poland*

(Dated: May 28, 2024)

We discuss entanglement and violation of Bell-type inequalities for a system of two Z bosons produced in Higgs decays. We take into account beyond the Standard Model (anomalous) coupling between H and daughter bosons but we limit ourselves to an overall scalar ZZ state (we exclude the possibility that H contains a pseudo-scalar component). In particular we consider the case when each Z decays further into fermion-antifermion pair. We find that the ZZ state is entangled and violates the CGLMP inequality for all values of the (anomalous) coupling constant. We also discuss the impact of a background on these results. The methods we develop are completely general, since they can be extrapolated to any scalar particle decaying into two spin-1 particles of different masses. Moreover, the violation of the CGLMP inequality in the final state is theoretically ensured for any value of the couplings.

I. INTRODUCTION

Violation of Bell inequalities is one of the most striking properties of quantum theory. Such a violation has been observed in a variety of physical systems like e.g. pairs of photons [1–3], ions [4], electrons [5], superconducting currents [6] or solid state systems [7].

Recently, the possibility of observing quantum entanglement and violation of Bell-type inequalities in high energy physics has been put forward. In particular, scattering processes [8, 9], systems of top quarks [10–15], $B^0\bar{B}^0$ mesons [16] and pairs of vector bosons arising from Higgs particle decay [17–22] were proposed in this context. This last possibility for the first time was suggested by Alan Barr in [17]. Barr considered there the violation of Clauser–Horn–Shimony–Holt (CHSH) and Collins–Gisin–Linden–Massar–Popescu (CGLMP) inequalities in a system of WW bosons arising in the decay of Higgs particle. In [18] the possible violation of CHSH, Mermin and CGLMP inequalities for a boson–antiboson system in an overall scalar state was discussed. In this paper the most general scalar state of two boson system was considered. If the bosons originate from the Higgs decay, then one of the components of such a general scalar state corresponds to an anomalous coupling of H with the daughter bosons (we explain this point in the present paper in Sec. II). Such a general scalar state of two vector bosons in the context of quantum correlations for the first time was discussed in [23] while the correlations of relativistic vector bosons in [24]. The authors of [19] analyzed entanglement and violation of CGLMP inequality

in the system of two Z bosons produced in the decay of a Higgs particle assuming the Standard Model interaction of H with the ZZ pair. In [21] entanglement of W bosons produced in $H \rightarrow WW \rightarrow l\nu l\nu$ channel was considered. The paper [20] explores the possibility of using quantum state tomography methods to determine a density matrix of massive particles produced in weak decays. In [22] entanglement and Bell inequality violation in boson pairs arising in the Standard Model processes $H \rightarrow WW^*$, $H \rightarrow ZZ^*$, $pp \rightarrow WW$, $pp \rightarrow WZ$, and $pp \rightarrow ZZ$ is considered.

In this paper we discuss entanglement and violation of the CGLMP inequality for a ZZ system produced in Higgs decay. We consider anomalous (beyond the Standard Model) structure of the vertex describing interaction of a Higgs particle with two daughter bosons but limit ourselves to the case of a scalar Higgs. Anomalous coupling parameters in the amplitude describing the interaction between H and ZZ bosons are strongly constrained by measurements of Higgs properties performed at the LHC [25], we discuss this point in detail in next section, below Eq. (9). However, our analysis is based on the most general Lorentz-covariant, CPT conserving amplitude (Eq. (8)) describing coupling of a (pseudo)scalar particle with two spin-1 particles with different masses. Thus, our considerations can be applied to each of such processes. The Higgs decay can be treated as an exemplary process of this kind.

It is also worth to notice the very recent papers [26, 27]. The authors of the former paper propose to use quantum tomography techniques to bound anomalous coupling in $H \rightarrow WW$ and $H \rightarrow ZZ$ decays while the authors of the latter one use entanglement to probe new physics in diboson production.

We use the standard units ($\hbar = c = 1$, here c stands for the velocity of light) and the Minkowski metric tensor

* alexander.bernal@csic.es

† Pawel.Caban@uni.lodz.pl (corresponding author)

‡ jaremb@uni.lodz.pl

$$\eta = \text{diag}(1, -1, -1, -1).$$

II. STATE OF THE TWO-BOSON SYSTEM ARISING FROM THE HIGGS DECAY

Our first goal is to construct a quantum state of two bosons arising in the process

$$H \rightarrow ZZ. \quad (1)$$

Let us denote by M the Higgs mass and by k, m_1 and p, m_2 the four-momenta and invariant masses of the in general off-shell Z bosons produced in the decay (1). In the actual decay of the Higgs particle into a pair of Z bosons typically one of them is nearly on-shell and the other one off-shell. Nevertheless, for the sake of generality, we consider Z bosons with arbitrary invariant masses. We decided to work in this framework as it covers all possible scenarios of a general on-shell scalar decaying into vector bosons. On the other hand, when we average the ZZ state over kinematical configurations we use the probability distribution $\mathcal{P}_c(m_1, m_2)$ (Eq. (32)) giving the probability that H decays into bosons with masses m_1 and m_2 . For the actual process (1) this probability density is peaked at $m_i = m_Z$ ($i = 1$ or 2). For further remarks on this point see the paragraph above Eq. (56). Moreover, we treat off-shell particles like ordinary on-shell particles with reduced masses. Similar approach has been applied in previous quantum-information-related studies [19, 22] as well as more phenomenologically-oriented papers like [28, 29].

We will perform our computations in the center of mass (CM) frame. In this frame we denote energies of Z bosons as ω_1 and ω_2 , consequently $k^\mu = (\omega_1, \mathbf{k})$, $p^\mu = (\omega_2, -\mathbf{k})$ and $\omega_1^2 - \mathbf{k}^2 = m_1^2$, $\omega_2^2 - \mathbf{k}^2 = m_2^2$.

Using similar notation as in [18, 23, 24], a general scalar state of two vector bosons with arbitrary masses can be written as

$$|\psi_{ZZ}^{\text{scalar}}(k, p)\rangle = g_{\mu\nu}(k, p)e_\lambda^\mu(k)e_\sigma^\nu(p)|\langle(k, \lambda); (p, \sigma)\rangle, \quad (2)$$

where

$$g_{\mu\nu}(k, p) = \eta_{\mu\nu} + \frac{c}{(kp)}(k_\mu p_\nu + p_\mu k_\nu), \quad c \in \mathbb{R}, \quad (3)$$

and $|\langle(k, \lambda); (p, \sigma)\rangle$ denotes the two-boson state, one boson with the four-momentum k and spin projection along z axis λ , second one with the four-momentum p and spin projection σ . The basis two-particle states fulfill the following orthogonality condition (for $k \neq p$) [30]:

$$\langle\langle(k, \lambda); (p, \sigma)|\langle(k, \lambda'); (p, \sigma')\rangle\rangle = \delta_{\lambda\lambda'}\delta_{\sigma\sigma'}. \quad (4)$$

The explicit form of amplitude $e_\lambda^\mu(q)$ for the four-momentum $q = (q^0, \mathbf{q})$ with $q^{02} - \mathbf{q}^2 = m^2$ reads [24]

$$e(q) = [e_\sigma^\mu(q)] = \begin{pmatrix} \frac{\mathbf{q}^T}{m} \\ \mathbb{I} + \frac{\mathbf{q} \otimes \mathbf{q}^T}{m(m+q^0)} \end{pmatrix} V^T, \quad (5)$$

and

$$V = \frac{1}{\sqrt{2}} \begin{pmatrix} -1 & i & 0 \\ 0 & 0 & \sqrt{2} \\ 1 & i & 0 \end{pmatrix}. \quad (6)$$

These amplitudes fulfill standard transversality condition

$$e_\sigma^\mu(q)q_\mu = 0. \quad (7)$$

To find an interpretation of the parameter c introduced in Eqs. (2,3) let us notice that the two boson state can be computed using the structure of the vertex describing interaction of the Higgs particle with two daughter vector bosons. Following e.g. [28, 29] the amplitude corresponding to the most general Lorentz-invariant, CPT conserving coupling of the (pseudo)scalar particle with two vector bosons can be cast in the following form:

$$\begin{aligned} \mathcal{A}_{\lambda\sigma}(k, p) \propto & [v_1\eta_{\mu\nu} + v_2(k+p)_\mu(k+p)_\nu \\ & + v_3\varepsilon_{\alpha\beta\mu\nu}(k+p)^\alpha(k-p)^\beta] e_\lambda^\mu(k)e_\sigma^\nu(p), \end{aligned} \quad (8)$$

where λ, σ are spin projections of the final states, v_1, v_2, v_3 are three real coupling constants, and $\varepsilon_{\alpha\beta\mu\nu}$ is a completely antisymmetric Levi-Civita tensor.

The Standard Model interaction corresponds to $v_1 = 1$, $v_2 = v_3 = 0$. On the other hand, $v_3 \neq 0$ implies that Higgs boson contains a pseudo-scalar component and indicates the possibility of CP violation. For the moment, let us consider the case $v_3 = 0$, $v_1 \neq 0$, and v_2 free. Comparing (2,3) with (8) and taking into account the transversality condition (7) we can relate the parameter c with the coupling constants v_1, v_2

$$c = \frac{v_2}{v_1}(kp). \quad (9)$$

Let us mention that the assumption $v_1 = 0$, apart from being unphysical (we know that the Higgs has $v_1 \neq 0$), together with $v_3 = 0$ leads to a separable state. Therefore, from now on we limit ourselves to the case $v_3 = 0$, $v_1 \neq 0$, v_2 free, that is we assume that the Higgs boson is a scalar but we admit a beyond Standard Model coupling $v_2 \neq 0$.

We would like to stress here that there exist experimental bounds on anomalous couplings v_2 and v_3 . Strong bound comes from the measurements of Higgs boson particles performed at the LHC by the CMS Collaboration [25]. The CMS Collaboration paper uses a different parametrization of the amplitude describing the interaction between H and two daughter bosons, instead of v_1, v_2 they use parameters a_1^{ZZ} and a_2^{ZZ} —see Eq. (2) in [25]. Comparing (2) in [25] and our Eq. (8) we obtain the following relation between the parameterizations:

$$v_1 \propto a_1^{ZZ} m_Z^2 + 2a_2^{ZZ}(kp), \quad v_2 \propto -2a_2^{ZZ} \quad (10)$$

(with the same proportionality constant). Thus, follow-

ing (9)

$$c = 2 \left(\frac{a_2^{ZZ}(kp)}{a_1^{ZZ} m_Z^2} \right) \frac{-1}{1 + 2 \left(\frac{a_2^{ZZ}(kp)}{a_1^{ZZ} m_Z^2} \right)} \Rightarrow$$

$$|c| = 2 \left| \frac{a_2^{ZZ}(kp)}{a_1^{ZZ} m_Z^2} \right| + \mathcal{O} \left(\left| \frac{a_2^{ZZ}(kp)}{a_1^{ZZ} m_Z^2} \right|^2 \right). \quad (11)$$

Now, the experimental bounds on the ratio a_2^{ZZ}/a_1^{ZZ} are given in Table 7 of [25] and in the on-shell case they read: $a_2^{ZZ}/a_1^{ZZ} \in [-0.12, 0.26]$ at 95% C.L. Thus, taking a larger value in this range, i.e. $|a_2^{ZZ}/a_1^{ZZ}| < 0.26$, and neglecting terms of order $|a_2^{ZZ}/a_1^{ZZ}|^2$ and higher, we get

$$|c| < 0.26 \frac{2(kp)}{m_Z^2}. \quad (12)$$

To estimate the maximal value of $2(kp)/m_Z^2$ we use Eq. (A5) and assume that one of the Z bosons is on-shell and the invariant mass of the off-shell Z boson is equal to zero. Inserting the measured values for the Higgs mass $M = 125.25$ GeV and Z mass $m_Z = 91.19$ GeV [31] we finally obtain the following bound for experimentally admissible values of c in the process $H \rightarrow ZZ$:

$$|c| < c_{\text{HZZ}}^{\text{max}} = 0.23. \quad (13)$$

Ref. [26] suggests that even stronger bound could be obtained using the tomography of the two-boson density matrix. Therefore, in the actual process $H \rightarrow ZZ$ the range of the parameter c which is not excluded by experimental data is rather narrow. However, as we mentioned in Introduction, the process $H \rightarrow ZZ$ can be treated as a model for the most general case of a decay of a (pseudo)scalar particle into two spin-1 particles with different masses. That is why in the following part of the paper we do not restrict values of c to the interval $(-c_{\text{HZZ}}^{\text{max}}, c_{\text{HZZ}}^{\text{max}})$.

The following comment is also in order here: when we consider a decay of a scalar particle into two gauge bosons, gauge invariance requires that v_2 coupling appears in the combination $v_2(k_\mu p_\nu - \eta_{\mu\nu}(kp))$ which is equivalent to $c = -1$. Thus, the cases $c = 0$ and $c = -1$ are indeed special as it was emphasized in [18].

The normalization of the scalar state defined in Eq. (2) is the following:

$$\langle \psi_{ZZ}^{\text{scalar}}(k, p) | \psi_{ZZ}^{\text{scalar}}(k, p) \rangle = A(k, p), \quad (14)$$

with

$$A(k, p) = 2 + \left[(1+c) \frac{(kp)}{m_1 m_2} - c \frac{m_1 m_2}{(kp)} \right]^2 \equiv 2 + \kappa^2, \quad (15)$$

where, for further convenience, we have introduced the parameter κ . Using formulas (A3-A7) we find that in the CM frame κ depends only on masses M, m_1, m_2 and the parameter c :

$$\kappa = \beta + c(\beta - 1/\beta), \quad (16)$$

where

$$\beta = \frac{M^2 - (m_1^2 + m_2^2)}{2m_1 m_2}. \quad (17)$$

The range of possible values of κ depends on the value of c and is the following:

$$\kappa \in (-\infty, 1] \quad \text{for } c \in (-\infty, -1), \quad (18)$$

$$\kappa \in [0, 1] \quad \text{for } c = -1, \quad (19)$$

$$\kappa \in [2\sqrt{-c(1+c)}, \infty) \quad \text{for } c \in (-1, -\frac{1}{2}), \quad (20)$$

$$\kappa \in [1, \infty] \quad \text{for } c \in [-\frac{1}{2}, \infty). \quad (21)$$

Nevertheless, further theoretical constraints must be taken into account to give the physically allowed range for c . In particular, perturbative unitarity (see [32] for a recent review applied to Higgs physics) imposes bounds over the values of the anomalous coupling v_2 . Namely, based on $ZZ \rightarrow ZZ$ scatterings, numerical bounds have been obtained for the $H \rightarrow ZZ$ anomalous couplings [33]. Comparing our amplitude (Eq. (8)) with Eq. (9) from [33] we get the following relation between our parametrization and parametrization used in [33]:

$$v_1 \propto a_1^{ZZH} m_Z^2 - a_2^{ZZH}(kp), \quad v_2 \propto a_2^{ZZH}. \quad (22)$$

Thus, following (9)

$$c = \left(\frac{a_2^{ZZH}(kp)}{a_1^{ZZH} m_Z^2} \right) \frac{1}{1 - \left(\frac{a_2^{ZZH}(kp)}{a_1^{ZZH} m_Z^2} \right)}. \quad (23)$$

Now, we use Eq. (A5) assuming that one of the Z bosons is on-shell and the invariant mass of the off-shell Z boson is equal to zero and apply Eqs. (11,12,25) from [33] to obtain

$$\frac{(kp)}{m_Z^2 a_1^{ZZH}} \cong 0.68158 \quad (24)$$

which gives

$$c \cong \frac{0.68158 a_2^{ZZH}}{1 - 0.68158 a_2^{ZZH}}. \quad (25)$$

Therefore, taking into account that according to Table I in [33]: $|a_2^{ZZH}| < 1.97$, we notice that c has a pole in the allowed range for a_2^{ZZH} and hence $c \in (-\infty, \infty)$. That is, we find that the requirement of perturbative unitarity does not limit accessible values of c in the process $H \rightarrow ZZ$.

Now, denoting

$$\mathbf{n} = \frac{\mathbf{k}}{|\mathbf{k}|}, \quad (26)$$

in the CM frame we can write the ZZ scalar state (2) as

$$|\psi_{ZZ}^{\text{scalar}}(m_1, m_2, \mathbf{n}, c)\rangle = \sum_{\lambda\sigma} \Omega_{\lambda\sigma}(k, \lambda; p, \sigma), \quad (27)$$

where $k^\mu = (\omega_1, 0, 0, |\mathbf{k}| \mathbf{n})$, $p^\mu = (\omega_2, 0, 0, -|\mathbf{k}| \mathbf{n})$, $\omega_1, \omega_2, |\mathbf{k}|$ are given by Eqs. (A6,A7,A4), respectively, and

$$\Omega = -\frac{1}{\sqrt{2+\kappa^2}} V(I + (\kappa-1)\mathbf{n} \otimes \mathbf{n}^T) V^T, \quad (28)$$

(V is defined in Eq. (6)).

Without loss of generality we take \mathbf{n} along z axis, $\mathbf{n} = (0, 0, 1)$ and simplify our notation:

$$|((\omega_1, 0, 0, |\mathbf{k}|), \lambda); ((\omega_2, 0, 0, -|\mathbf{k}|), \sigma)\rangle \equiv |\lambda, \sigma\rangle. \quad (29)$$

With such a choice we have

$$\Omega = \frac{1}{\sqrt{2+\kappa^2}} \begin{pmatrix} 0 & 0 & 1 \\ 0 & -\kappa & 0 \\ 1 & 0 & 0 \end{pmatrix}, \quad (30)$$

and the explicit form of the ZZ state in this case reads

$$|\psi_{ZZ}^{\text{scalar}}(m_1, m_2, c)\rangle = \frac{1}{\sqrt{2+\kappa^2}} \left[|+, -\rangle - \kappa |0, 0\rangle + |-, +\rangle \right]. \quad (31)$$

It is worth taking note that the form of the above state agrees with the most general form of the ZZ state arising in the $H \rightarrow ZZ$ process conserving parity—compare Eq. (7) from [19]. Moreover, when we put $c = 0$ in Eq. (16) the state (31) coincides with the ZZ state discussed in [19] where only the Standard Model vertex has been considered.

A. Averaging over kinematical configurations

In the realistic case when the state is determined on the basis of data obtained from various kinematical configurations, one has to average over these configuration. Thus, in such a case we receive a mixed state which for a given c reads

$$\rho_{ZZ}(c) = \int dm_1 dm_2 \mathcal{P}_c(m_1, m_2) \rho(m_1, m_2, c), \quad (32)$$

where $\rho(m_1, m_2, c) = |\psi_{ZZ}^{\text{scalar}}(m_1, m_2, c)\rangle \langle \psi_{ZZ}^{\text{scalar}}(m_1, m_2, c)|$ (c.f. (31)) and $\mathcal{P}_c(m_1, m_2)$ is a normalized probability distribution. To determine the form of $\mathcal{P}_c(m_1, m_2)$, we assume that each of the Z bosons produced in the process (1) decays subsequently into massless fermion–antifermion pair, i.e. we consider the process

$$H \rightarrow ZZ \rightarrow f_1^+ f_1^- f_2^+ f_2^-. \quad (33)$$

The normalized differential cross section of the decay $ZZ \rightarrow f_1^+ f_1^- f_2^+ f_2^-$ is given by

$$\frac{1}{\sigma} \frac{d\sigma}{d\Omega_1 d\Omega_2} = \left(\frac{3}{4\pi}\right)^2 \text{Tr} [\rho_{ZZ}(c) (\Gamma_1^T \otimes \Gamma_2^T)], \quad (34)$$

where Γ_i is the decay matrix of $Z_i \rightarrow f_i^+ f_i^-$, Ω_i is the solid angle related to the final particle f_i [19, 34]. Now,

inserting (32) into (34), integrating with respect to solid angles, using the property that $\int \Gamma_i d\Omega_i = \frac{4\pi}{3} I$, and differentiating with respect to m_1, m_2 we obtain

$$\frac{1}{\sigma} \frac{d\sigma}{dm_1 dm_2}(m_1, m_2, c) = \frac{\mathcal{P}_c(m_1, m_2)}{\text{Tr}[\tilde{\rho}(m_1, m_2, c)]} \text{Tr}[\tilde{\rho}(m_1, m_2, c)], \quad (35)$$

where by $\tilde{\rho}(m_1, m_2, c)$ we have denoted non-normalized density matrix $\rho(m_1, m_2, c)$, i.e.,

$$\tilde{\rho}(m_1, m_2, c) = \left[|+, -\rangle - \kappa |0, 0\rangle + |-, +\rangle \right] \times \left[\langle +, -| - \kappa \langle 0, 0| + \langle -, +| \right]. \quad (36)$$

Next, Eq. (8) from [29] in our notation can be written as[35]

$$\frac{1}{\sigma} \frac{d\sigma}{dm_1 dm_2}(m_1, m_2, c) = N \frac{\lambda^{1/2}(M^2, m_1^2, m_2^2) m_1^3 m_2^3}{D(m_1) D(m_2)} \text{Tr}[\tilde{\rho}(m_1, m_2, c)], \quad (37)$$

where N is a normalization factor independent of m_1, m_2 and c ; while the functions λ and D are defined in Eqs. (A1,A2). Comparing (35) with (37) (and taking into account (36)) we finally obtain the probability distribution

$$\mathcal{P}_c(m_1, m_2) = N \frac{\lambda^{1/2}(M^2, m_1^2, m_2^2) m_1^3 m_2^3}{D(m_1) D(m_2)} [2 + \kappa^2]. \quad (38)$$

For a given value of c the normalization factor N can be determined numerically. In [19] the probability distribution $\mathcal{P}_{c=0}(m_1, m_2)$ has been obtained with the help of Monte Carlo simulation. The results coincide with those computed from (38).

Therefore, using (16,32,38), the density matrix averaged over kinematical configurations can be written as

$$\rho_{ZZ}(c) = \frac{1}{2a+b} \begin{pmatrix} 0 & 0 & 0 & 0 & 0 & 0 & 0 & 0 & 0 \\ 0 & 0 & 0 & 0 & 0 & 0 & 0 & 0 & 0 \\ 0 & 0 & \boxed{a} & 0 & \boxed{-d} & 0 & \boxed{a} & 0 & 0 \\ 0 & 0 & 0 & 0 & 0 & 0 & 0 & 0 & 0 \\ 0 & 0 & \boxed{-d} & 0 & \boxed{b} & 0 & \boxed{-d} & 0 & 0 \\ 0 & 0 & 0 & 0 & 0 & 0 & 0 & 0 & 0 \\ 0 & 0 & \boxed{a} & 0 & \boxed{-d} & 0 & \boxed{a} & 0 & 0 \\ 0 & 0 & 0 & 0 & 0 & 0 & 0 & 0 & 0 \\ 0 & 0 & 0 & 0 & 0 & 0 & 0 & 0 & 0 \end{pmatrix}, \quad (39)$$

where for better visibility we have framed the non-zero matrix elements:

$$a = \mathbf{B}(0), \quad (40)$$

$$b = \mathbf{B}(2) + 2c[\mathbf{B}(2) - \mathbf{B}(0)] + c^2[\mathbf{B}(2) + \mathbf{B}(-2) - 2\mathbf{B}(0)], \quad (41)$$

$$d = \mathbf{B}(1) + c[\mathbf{B}(1) - \mathbf{B}(-1)], \quad (42)$$

and we have introduced the following notation

$$\mathbf{B}(n) = \int_{0 \leq m_1 + m_2 \leq M} dm_1 dm_2 \frac{\lambda^{1/2}(M^2, m_1^2, m_2^2) m_1^3 m_2^3}{D(m_1)D(m_2)} \beta^n, \quad (43)$$

for $n = -2, -1, 0, 1, 2$.

Note that sometimes it is relevant for phenomenological purposes to implement cuts on the possible values of the boson masses (for example to remove part of the background of a certain scattering process). This feature is easily implemented theoretically via the integrals defining $\mathbf{B}(n)$. For instance, when considering a lower cut in the off-shell mass of the vector boson, $m_i \geq m_i^{\text{cut}}$, one just needs to modify the lower bound in the integral over the corresponding mass:

$$\begin{aligned} \int_{0 \leq m_1 + m_2 \leq M} dm_1 dm_2 &= \int_0^M dm_1 \int_0^{M-m_1} dm_2 \\ &\rightarrow \int_{m_1^{\text{cut}}}^M dm_1 \int_{m_2^{\text{cut}}}^{M-m_1} dm_2. \end{aligned} \quad (44)$$

When we insert the measured values for the Higgs mass, Z mass and Z decay width, i.e., $M = 125.25$ GeV, $m_Z = 91.19$ GeV, $\Gamma_Z = 2.50$ GeV [31] we obtain

$$a_Z = 2989.76, \quad (45)$$

$$b_Z = 9431.55 + 12883.6c + 4983.07c^2, \quad (46)$$

$$d_Z = 4819.07 + 2752.19c. \quad (47)$$

III. BELL INEQUALITIES AND ENTANGLEMENT

Now, we are at a position to discuss the violation of Bell inequalities in a system of two ZZ bosons. Various Bell inequalities have been designed for detecting departures from local realism by quantum mechanical systems [36], the most popular one being the CHSH inequality [37]. For a system consisting of two d -dimensional subsystems the optimal Bell inequality was formulated in [38, 39] and is known as the CGLMP inequality. For two qubits it reduces to the CHSH inequality. We consider here two spin-1 particles therefore we present the CGLMP inequality for $d = 3$. We assume that Alice (Bob) can perform two possible measurements A_1 or A_2 (B_1 or B_2) on her (his) subsystem, respectively. Each of these measurements can have three outcomes: 0,1,2. Let $P(A_i = B_j + k)$ denotes the probability that the outcomes A_i and B_j differ by k modulo 3, i.e., $P(A_i = B_j + k) = \sum_{l=0}^{2-k} P(A_i = l, B_j = l + k \pmod{3})$, and let us define the following quantity

$$\begin{aligned} \mathcal{I}_3 &= [P(A_1 = B_1) + P(B_1 = A_2 + 1) \\ &\quad + P(A_2 = B_2) + P(B_2 = A_1)] \\ &\quad - [P(A_1 = B_1 - 1) + P(B_1 = A_2) \\ &\quad + P(A_2 = B_2 - 1) + P(B_2 = A_1 - 1)]. \end{aligned} \quad (48)$$

The CGLMP inequality has the form

$$\mathcal{I}_3 \leq 2. \quad (49)$$

We assume that Alice can perform measurements on one of the Z bosons, Bob on the second one. In principle, what they can measure are spin projections on given directions. A few remarks are in order here. In [18] we discussed broader the problem of choice of the proper spin observable. We have advocated there the Newton–Wigner spin operator. Under our assumptions, when Alice applies this spin operator to the basis vector $|\lambda, \sigma\rangle$, this action can be written as the action of $(\mathbf{S}_{\lambda\lambda} \otimes I)$ on $|\lambda'\rangle \otimes |\sigma\rangle$, where S^i are standard spin-1 matrices (and analogously for Bob). Therefore, from now on we take Alice (Bob) observables as $A \otimes I$ ($I \otimes B$) and identify $|\lambda\rangle \otimes |\sigma\rangle \equiv |\lambda, \sigma\rangle$.

A. Probabilities of spin projection measurements for a particular configuration

In general, when discussing the violation of CGLMP inequality by the state $\rho_{ZZ}(c)$ (Eq. (39)) we do not restrict our attention to spin projection measurements only. However, for a particular configuration, the probabilities $P_{\lambda\sigma}$ that Alice and Bob receive λ and σ when they measure spin projections along directions \mathbf{a} and \mathbf{b} in the pure state (27), respectively, can be calculated explicitly. We present them below

$$\begin{aligned} P_{\pm\pm} &= \frac{1}{4[2 + \kappa^2]} \left\{ [1 - (\mathbf{a} \cdot \mathbf{b})]^2 \right. \\ &\quad + 2(\kappa - 1)[1 - (\mathbf{a} \cdot \mathbf{b}) + (1 + (\mathbf{a} \cdot \mathbf{b}))(\mathbf{a} \cdot \mathbf{n})(\mathbf{b} \cdot \mathbf{n}) - (\mathbf{a} \cdot \mathbf{n})^2 \\ &\quad \left. - (\mathbf{b} \cdot \mathbf{n})^2] + (\kappa - 1)^2 [1 - (\mathbf{a} \cdot \mathbf{n})^2][1 - (\mathbf{b} \cdot \mathbf{n})^2] \right\}, \end{aligned} \quad (50)$$

$$\begin{aligned} P_{\pm\mp} &= \frac{1}{4[2 + \kappa^2]} \left\{ [1 + (\mathbf{a} \cdot \mathbf{b})]^2 \right. \\ &\quad + 2(\kappa - 1)[1 + (\mathbf{a} \cdot \mathbf{b}) - (1 - (\mathbf{a} \cdot \mathbf{b}))(\mathbf{a} \cdot \mathbf{n})(\mathbf{b} \cdot \mathbf{n}) - (\mathbf{a} \cdot \mathbf{n})^2 \\ &\quad \left. - (\mathbf{b} \cdot \mathbf{n})^2] + (\kappa - 1)^2 [1 - (\mathbf{a} \cdot \mathbf{n})^2][1 - (\mathbf{b} \cdot \mathbf{n})^2] \right\}, \end{aligned} \quad (51)$$

$$\begin{aligned} P_{0\pm} &= \frac{1}{2[2 + \kappa^2]} \left\{ 1 + (\kappa^2 - 1)(\mathbf{a} \cdot \mathbf{n})^2 \right. \\ &\quad \left. - [(\mathbf{a} \cdot \mathbf{b}) + (\kappa - 1)(\mathbf{a} \cdot \mathbf{n})(\mathbf{b} \cdot \mathbf{n})]^2 \right\}, \end{aligned} \quad (52)$$

$$\begin{aligned} P_{\pm 0} &= \frac{1}{2[2 + \kappa^2]} \left\{ 1 + (\kappa^2 - 1)(\mathbf{b} \cdot \mathbf{n})^2 \right. \\ &\quad \left. - [(\mathbf{a} \cdot \mathbf{b}) + (\kappa - 1)(\mathbf{a} \cdot \mathbf{n})(\mathbf{b} \cdot \mathbf{n})]^2 \right\}, \end{aligned} \quad (53)$$

$$P_{00} = \frac{1}{2 + \kappa^2} [(\mathbf{a} \cdot \mathbf{b}) + (\kappa - 1)(\mathbf{a} \cdot \mathbf{n})(\mathbf{b} \cdot \mathbf{n})]^2. \quad (54)$$

For the case $m_1 = m_2$ the above probabilities coincide with the probabilities found in [18].

It is worth noticing that if Alice and Bob are allowed to use only spin projections as observables then, in principle, the violation of the Bell inequality would be suboptimal as we are not covering the whole space of possible observables.

B. Bell inequalities in a general ZZ state

Now, we want to answer the question whether the state (39) violates the CGLMP inequality. In general, for a given state ρ there does not exist a simple way to find optimal observables A_1, A_2, B_1, B_2 , i.e., such observables for which the value of \mathcal{I}_3 is maximal in the state ρ . Usually, optimal observables are looked for with the help of a certain optimization procedure. In [19] such a procedure was proposed in the considered there Standard Model coupling case, i.e. for $c = 0$. In this procedure one modifies the well known optimal choice of observables for the maximally entangled state. For completeness we describe the details of this procedure in B 1. This procedure works very well for the case $c = 0$ and for c close to that value. However, for higher values of $|c|$ this procedure gives the observables which do not violate the CGLMP inequality.

Thus, we have considered also a different optimization procedure. This procedure is inspired by the proof of Theorem 2 in [40]. The details of this approach we described in B 2.

In Fig. 1 we present the maximal value of \mathcal{I}_3 as a function of c obtained with the help of both mentioned above optimization strategies. This plot shows that the state $\rho_{ZZ}(c)$ can violate the CGLMP inequality (39) for all values of c . For $c \in (c_-^Z, c_+^Z)$, where $c_-^Z = -1.3749$, $c_+^Z = 1.6690$, the optimization procedure proposed in [19] gives higher violation of CGLMP inequality than the procedure proposed in B 2. For other values of c the situation is opposite. The highest value of \mathcal{I}_3 we obtained is equal to 2.9047, it is attained for $c_{\max}^Z = -0.8536$.

Regarding the values $|c| < c_{\text{HZZ}}^{\max}$, larger violation of order [2.5, 2.8] is obtained when the optimization strategy from B 1 is implemented, while violations of order [2.2, 2.3] are attained for the optimization presented in B 2.

C. Entanglement of a general ZZ state

To evaluate entanglement of the state (39) we use the computable entanglement measure called logarithmic negativity [41, 42]

$$E_N(\rho) = \log_3(\|\rho^{T_B}\|_1), \quad (55)$$

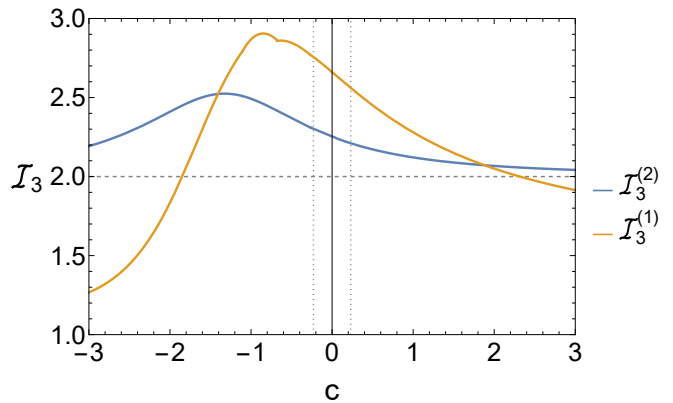


FIG. 1: In this figure we present the maximal value of \mathcal{I}_3 in the state (39) as a function of c . We have inserted the measured values for the Higgs mass, Z mass and Z decay width, i.e., we put a, b, d given in Eqs. (45,46,47). The $\mathcal{I}_3^{(1)}$ curve was obtained with the help of the optimization procedure described in B 1 while the curve $\mathcal{I}_3^{(2)}$ with the help of the procedure from B 2. Vertical dotted lines delimit the range $(-c_{\text{HZZ}}^{\max}, c_{\text{HZZ}}^{\max})$ (with $c_{\text{HZZ}}^{\max} = 0.26$ —compare Eq. (13)) of the parameter c admissible by experimental data for the process $H \rightarrow ZZ$.

where $\|A\|_1 = \text{Tr}(\sqrt{A^\dagger A})$ is the trace norm of a matrix A and T_B denotes partial transposition with respect to the second subsystem. The trace norm of a matrix A is equal to the sum of all the singular values of A ; when A is hermitian then $\|A\|_1$ is equal to the sum of absolute values of all eigenvalues of A .

If a state ρ is separable then the logarithmic negativity of ρ is equal to zero. Thus, $E_N(\rho) > 0$ indicates that the state ρ is entangled. In Fig. 2 we have plotted the logarithmic negativity of the state (39) with a_Z, b_Z , and d_Z given in Eqs. (45,46,47). We see that the state is entangled for all values of c , the maximal value of the logarithmic negativity equal to 0.9964 is attained for $c = -0.7371$. It is worth noticing that the state with the highest entanglement corresponds to $c = -0.7371$ while the state with the highest violation of the CGLMP inequality corresponds to $c = -0.8536$, i.e., these states are different. This observation is consistent with the general property of CGLMP inequality [43].

Concerning the logarithmic negativity for $|c| < c_{\text{HZZ}}^{\max}$, it this is considerably far apart from 0, within a range $\sim [0.85, 0.95]$. This indicates a high grade of entanglement in any ZZ pair stemming from Higgs decays.

D. Impact of a background

Because the reconstruction of $\rho_{ZZ}(c)$ in a collider experiment is done via quantum tomography methods [19, 20, 44], the presence of systematic and statistical errors as well as the existence of a small background in

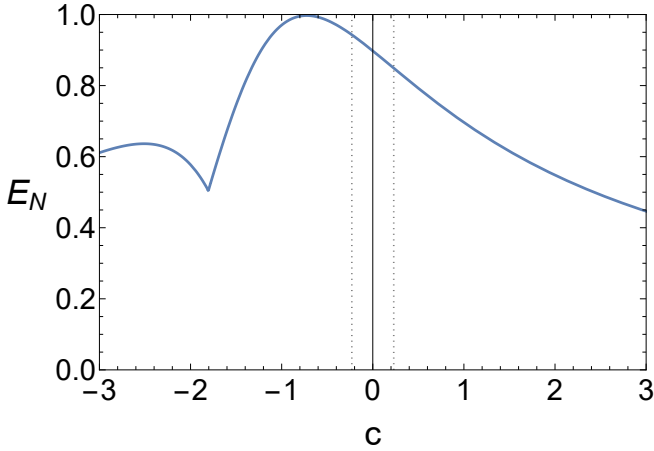


FIG. 2: In this figure we present logarithmic negativity of the state (39), $E_N(\rho_{ZZ}(c))$ as a function of c . We have inserted the measured values for the Higgs mass, Z mass and Z decay width, i.e., we put a, b, d given in Eqs. (45,46,47). The cusp occurs for the value of c for which the parameter d_Z in the density matrix vanishes and is caused by the change in monotonicity of the trace norm of the partially transposed matrix. Vertical dotted lines delimit the range $(-c_{\text{HZZ}}^{\text{max}}, c_{\text{HZZ}}^{\text{max}})$ (with $c_{\text{HZZ}}^{\text{max}} = 0.26$ —compare Eq. (13)) of the parameter c admissible by experimental data for the process $H \rightarrow ZZ$.

$H \rightarrow ZZ \rightarrow f_1^+ f_1^- f_2^+ f_2^-$ processes lead to a modification of its exact form. Following the discussion given in [19], we will focus on analyzing $H \rightarrow ZZ \rightarrow e^+ e^- \mu^+ \mu^-$, since it constitutes one of the cleanest channels to be explored at the LHC. In principle, the two Z bosons are cleanly identified. Due to the fact that one of them is nearly on-shell, it gives two leptons whose invariant mass is close to m_Z , while the remaining two leptons have a much lower invariant mass. We have labeled the (very close to real) Z boson with largest invariant mass as Z_1 and its four-momentum could be reconstructed from its decay products $l_1^+ l_1^-$. On the other hand, the off-shell Z boson is labeled as Z_2 and its momentum is determined summing up the momenta of its decay products $l_2^+ l_2^-$.

Concerning both the systematic and statistical errors of the tomography procedure, it was stated in [19] that the statistical one dominates with respect to the systematics and detector resolution. An estimation of the former was computed in this previous paper and the results show that, even with these errors, a violation of Bell inequalities for the $\rho_{ZZ}(0)$ state could be probed at the 4.5σ level in the HL-LHC. Regarding the background of the process, the main one comes from the electroweak one $pp \rightarrow ZZ/Z\gamma \rightarrow 4l$, being this one about 4 times smaller at the Higgs peak [45]. Nevertheless, as claimed in [19], a background subtraction will be necessary before computing the entanglement observable and evaluating the CGLMP inequality. In general, the non-negligible background will slightly contribute to the sta-

tistical uncertainty of the measurements. Moreover, as proposed in [19], the larger the invariant mass m_2 of the off-shell Z boson, the more entangled the $\rho_{ZZ}(c)$ state. Therefore, requiring a lower cut on m_2 leads to an interplay between increasing the entanglement (hence the violation of the CGLMP inequality) and decreasing the statistics (thus increasing the uncertainty in the measurements). In Figs. 3, 4, 5 we have studied the theoretical dependence of \mathcal{I}_3 and E_N on c , once the cuts $m_2 \geq 0, 10, 20, 30$ GeV are implemented.

Returning for a moment to our discussion of “off-shellness” of Z bosons produced in the decay (1), let us notice that $\mathcal{I}_3^{(1)}$ and $\mathcal{I}_3^{(2)}$ obtained for $m_1 = m_Z$, $0 \text{ GeV} \leq m_2 \leq m_H - m_Z$ (blue curves in Figs. 3 and 4) are identical as $\mathcal{I}_3^{(1)}$ and $\mathcal{I}_3^{(2)}$ plotted in Fig. 1 where we allowed arbitrary masses m_1 and m_2 (of course constrained by the four-momentum conservation). The same holds for E_N plotted in Figs. 5 (blue line) and 2. Of course this coincidence is not accidental, it results from the fact that the probability distribution $\mathcal{P}_c(m_1, m_2)$ is peaked at $m_i = m_Z$.

Finally, in order to estimate the overall allowed uncertainty in both the entanglement and the Bell inequality violation, we have estimated the noise resistance of the CGLMP inequality violation with respect to the white noise. To this aim we considered the state $\rho_{ZZ}(c)$ mixed with the identity operator, i.e. the state

$$\lambda \rho_{ZZ}(c) + (1 - \lambda) \frac{1}{9} I_9, \quad \lambda \in (0, 1]. \quad (56)$$

Now, the noise resistance we define as a minimal value of λ , λ_{min} , for which the state (56) violates the CGLMP inequality. Inserting the state (56) into the CGLMP inequality (B1) and taking into account that $\text{Tr}(\mathcal{O}_{\text{Bell}}) = 0$ we obtain

$$\lambda_{\text{min}} = \frac{2}{\max\{\text{Tr}(\rho_{ZZ}(c)\mathcal{O}_{\text{Bell}})\}}. \quad (57)$$

We obtained the maximal value of $\text{Tr}(\rho_{ZZ}(c)\mathcal{O}_{\text{Bell}}) = \mathcal{I}_3$ with the help of two different optimization procedures (B1 and B2) and denoted as $\mathcal{I}_3^{(1)}$ and $\mathcal{I}_3^{(2)}$, respectively (compare Fig. 1). Therefore, we have

$$\lambda_{\text{min}} = \frac{2}{\max\{\mathcal{I}_3^{(1)}, \mathcal{I}_3^{(2)}\}} \quad (58)$$

and this value we have plotted in Fig. 6.

The plots show that for values of c close to 0 (which are the expected ones, due to the present bounds in anomalous couplings for the HZZ vertex [46]), one can stand up to almost a 20% of noise and still attain a violation of the CGLMP inequality and hence an entangled state. Actually, the resistance to noise increases with the invariant mass of the off-shell Z boson, reaching for the cut $m_2 \geq 30$ GeV a resistance of 20% for $c \in [-3, 3]$ and a resistance of almost 30% for $c \in [-2, 2]$.

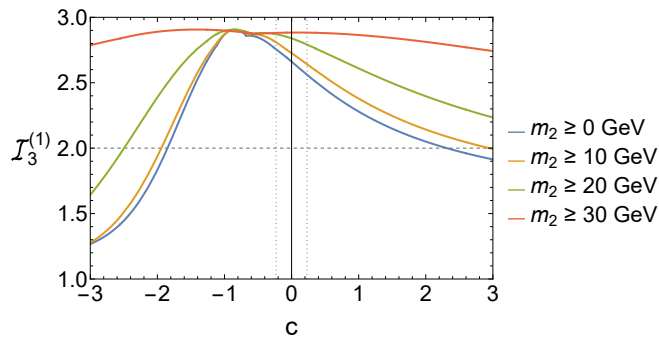


FIG. 3: In this figure we present the maximal value of \mathcal{I}_3 in the state (39) as a function of c . We have inserted the measured values for the Higgs mass, Z mass and Z decay width, i.e., we put a, b, d given in Eqs. (45,46,47). We have applied the optimization procedure described in B1 and assumed the cuts $m_2 \geq 0, 10, 20, 30$ GeV are implemented. Vertical dotted lines delimit the range $(-c_{\text{HZZ}}^{\text{max}}, c_{\text{HZZ}}^{\text{max}})$ (with $c_{\text{HZZ}}^{\text{max}} = 0.26$ —compare Eq. (13)) of the parameter c admissible by experimental data for the process $H \rightarrow ZZ$.

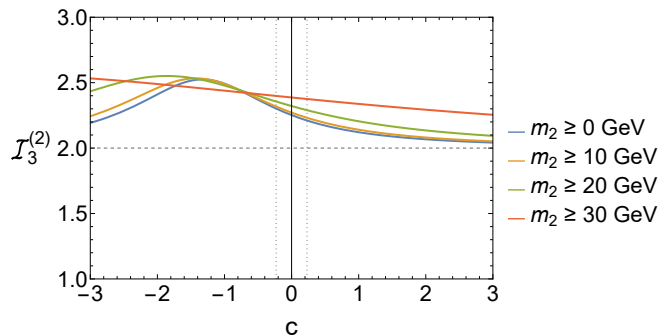


FIG. 4: In this figure we present the maximal value of \mathcal{I}_3 in the state (39) as a function of c . We have inserted the measured values for the Higgs mass, Z mass and Z decay width, i.e., we put a, b, d given in Eqs. (45,46,47). We have applied the optimization procedure described in B2 and assumed the cuts $m_2 \geq 0, 10, 20, 30$ GeV are implemented. Vertical dotted lines delimit the range $(-c_{\text{HZZ}}^{\text{max}}, c_{\text{HZZ}}^{\text{max}})$ (with $c_{\text{HZZ}}^{\text{max}} = 0.26$ —compare Eq. (13)) of the parameter c admissible by experimental data for the process $H \rightarrow ZZ$.

IV. CONCLUSIONS

In conclusions, we have analyzed entanglement and Bell inequality violation in a system of two Z bosons produced in Higgs decay. We consider beyond the Standard Model structure of the vertex describing interaction of H with daughter bosons. The amplitude corresponding to the most general Lorentz-invariant, CPT conserving coupling of a (pseudo)scalar particle with two vector bosons depends on three coupling constants v_1, v_2, v_3 , and is explicitly given in Eq. (8). The Standard Model interaction corresponds to $v_1 = 1, v_2 = v_3 = 0$ while

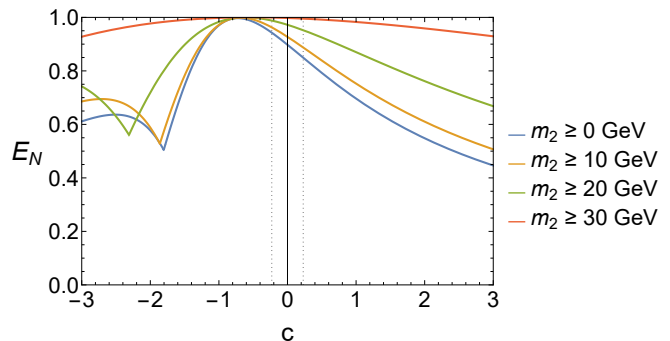


FIG. 5: In this figure we present logarithmic negativity of the state (39), $E_N(\rho_{ZZ}(c))$ as a function of c . We have inserted the measured values for the Higgs mass, Z mass and Z decay width, i.e., we put a, b, d given in Eqs. (45,46,47). We have assumed the cuts $m_2 \geq 0, 10, 20, 30$ GeV are implemented. Vertical dotted lines delimit the range $(-c_{\text{HZZ}}^{\text{max}}, c_{\text{HZZ}}^{\text{max}})$ (with $c_{\text{HZZ}}^{\text{max}} = 0.26$ —compare Eq. (13)) of the parameter c admissible by experimental data for the process $H \rightarrow ZZ$.

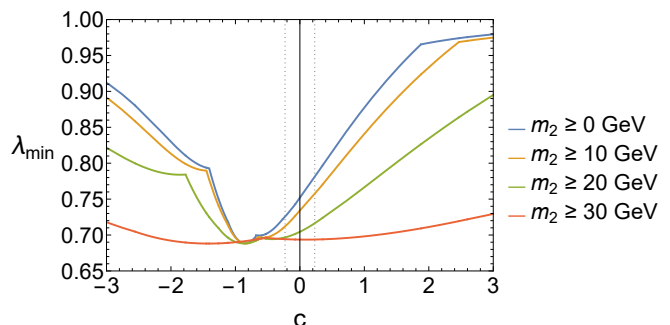


FIG. 6: In this figure we present λ_{min} (58), as a function of c . We have inserted the measured values for the Higgs mass, Z mass and Z decay width, i.e., we put a, b, d given in Eqs. (45,46,47). We have assumed the cuts $m_2 \geq 0, 10, 20, 30$ GeV are implemented. Vertical dotted lines delimit the range $(-c_{\text{HZZ}}^{\text{max}}, c_{\text{HZZ}}^{\text{max}})$ (with $c_{\text{HZZ}}^{\text{max}} = 0.26$ —compare Eq. (13)) of the parameter c admissible by experimental data for the process $H \rightarrow ZZ$.

$v_3 \neq 0$ implies Higgs boson with a pseudo-scalar component and indicates the possibility of CP violation. In this paper we have considered the case $v_3 = 0, v_1 \neq 0, v_2$ free, i.e. we have assumed the scalar Higgs boson but admitted a beyond Standard Model coupling $v_2 \neq 0$. In such a case, the state of produced bosons, beyond four-momenta and spins, can be characterized by a single parameter c which, up to normalization is equal to v_2/v_1 (compare Eq. (9)). Under such assumptions, in the center-of-mass frame, we have determined the most general state of ZZ boson pair for a particular event $H \rightarrow ZZ$. Next, we have considered a more realistic case when data are collected from different kinematical configurations. In such a sit-

uation a ZZ state can be calculated by averaging over those configurations with respect to a proper probability distribution function (PDF). Thus, assuming further that each Z boson decays into fermion-antifermion pair, we have derived the corresponding PDF and computed the ZZ boson density matrix. Finally, we have shown that this matrix is entangled and violates the CGLMP inequality for all values of coupling (i.e. for all values of c) including the range admissible by experimental data [25]. The procedure to check this is completely general and can be applied for any other decay of a scalar particle into vector bosons, with their corresponding decay to fermions, once the PDF of the latter decay is known.

Moreover, our preliminary studies show that the inclusion of a CP-odd anomalous coupling should not qualitatively change the results derived. However, in this case the optimization strategy is more involved and work is still in progress.

Summarizing, this work settles a constructive way of probing the entanglement and violation of Bell inequalities of any vector boson pair coming from a spin-0 particle, independently of the value of the couplings in hand (as long as the interactions among particles are CPT and Lorentz invariant). This feature is of a complete novelty in the literature and states the highly non-trivial fact that non locality (and hence entanglement) of vector bosons in these kinds of processes is theoretical ensured in any phenomenological model (it could have been the case in which although the state is entangled, it does not violate any Bell inequality). Thus, the only limitation in checking the quantum behavior of these processes comes from the experimental side. In particular, this work gives the theoretical framework to test the quantum nature of processes in a great variety of phenomenological models, covering for instance models with extended scalar sectors as well as axion like particles (ALP) models where we let the ALP to interact with vector bosons.

ACKNOWLEDGMENTS

P.C. and J.R. are supported by the University of Lodz under IDUB project. A.B. is grateful to J.A. Casas and J. M. Moreno for very useful discussions. A.B. acknowledges the support of the Spanish Agencia Estatal de Investigacion through the grants ‘‘IFT Centro de Excelencia Severo Ochoa CEX2020-001007-S’’ and PID2019-110058GB-C22 funded by MCIN/AEI/10.13039/501100011033 and by ERDF. The work of A.B. is supported through the FPI grant PRE2020-095867 funded by MCIN/AEI/10.13039/501100011033.

Appendix A: Some definitions and useful formulas

Following e.g. [29] we define the following functions

$$\lambda(x, y, z) = x^2 + y^2 + z^2 - 2xy - 2xz - 2yz, \quad (\text{A1})$$

$$D(m) = (m^2 - m_Z^2)^2 + (m_Z \Gamma_Z)^2, \quad (\text{A2})$$

where m_Z, Γ_Z denotes the mass and decay width of the on-shell Z boson. In the CM frame the Higgs particle with the four-momentum $(M, \mathbf{0})$ decays into two off-shell Z bosons with four-momenta $k^\mu = (\omega_1, \mathbf{k}), \omega_1^2 - \mathbf{k}^2 = m_1^2$ and $p^\mu = (\omega_2, -\mathbf{k}), \omega_2^2 - \mathbf{k}^2 = m_2^2$. The energy conservation gives

$$M = \omega_1 + \omega_2. \quad (\text{A3})$$

Using these equations in the CM frame we obtain

$$\mathbf{k}^2 = \frac{1}{4M^2} \lambda(M^2, m_1^2, m_2^2), \quad (\text{A4})$$

$$kp = \frac{1}{2} [M^2 - m_1^2 - m_2^2], \quad (\text{A5})$$

$$\omega_1 = \frac{1}{2M} [M^2 + (m_1^2 - m_2^2)], \quad (\text{A6})$$

$$\omega_2 = \frac{1}{2M} [M^2 - (m_1^2 - m_2^2)]. \quad (\text{A7})$$

Appendix B: Optimal observables for CGLMP violation

For completeness we describe here the optimization strategies used to obtain observables $A_1, A_2, B_1,$ and B_2 which maximize the value of \mathcal{I}_3 as depicted in Fig. 1.

The first procedure is similar to that applied in [19]. The second one is inspired by the proof of Theorem 2 in [40].

First, it is clear that the CGLMP inequality (49) can be written as

$$\text{Tr}(\rho \mathcal{O}_{\text{Bell}}) \leq 2, \quad (\text{B1})$$

where $\mathcal{O}_{\text{Bell}}$ is a certain operator depending on the observables $A_1, A_2, B_1,$ and B_2 .

Next, each hermitian 3×3 observable A can be represented via the 3×3 unitary matrix U_A . This unitary matrix is defined in a simple way: columns of U_A are normalized eigenvectors of A in a given basis. With this notation one obtains [19]

$$\begin{aligned} \mathcal{O}_{\text{Bell}} = & -[U_{A_1} \otimes U_{B_1}] P_1 [I \otimes S^3] P_1^\dagger [U_{A_1} \otimes U_{B_1}]^\dagger \\ & + [U_{A_1} \otimes U_{B_2}] P_0 [I \otimes S^3] P_0^\dagger [U_{A_1} \otimes U_{B_2}]^\dagger \\ & + [U_{A_2} \otimes U_{B_1}] P_1 [I \otimes S^3] P_1^\dagger [U_{A_2} \otimes U_{B_1}]^\dagger \\ & - [U_{A_2} \otimes U_{B_2}] P_1 [I \otimes S^3] P_1^\dagger [U_{A_2} \otimes U_{B_2}]^\dagger, \end{aligned} \quad (\text{B2})$$

where S^3 is the standard spin z component matrix, $S^3 = \text{diag}(1, 0, -1)$, and P_0, P_1 are $3^2 \times 3^2$ block-diagonal

permutation matrices:

$$P_n = \begin{pmatrix} C^n & \mathcal{O} & \mathcal{O} \\ \mathcal{O} & C^{n+1} & \mathcal{O} \\ \mathcal{O} & \mathcal{O} & C^{n+2} \end{pmatrix}, \quad n = 0, 1, \quad (\text{B3})$$

where \mathcal{O} is the 3×3 null matrix and C is the 3×3 cyclic permutation matrix

$$C = \begin{pmatrix} 0 & 0 & 1 \\ 1 & 0 & 0 \\ 0 & 1 & 0 \end{pmatrix}. \quad (\text{B4})$$

Each U from (B2) can be taken as an element of $SU(3)$ group, this group has 8 parameters. Thus, to perform the full optimization of $\mathcal{O}_{\text{Bell}}$ for a given state one should check the 8^4 dimensional parameter space.

1. Strategy 1

To simplify this task, in [19] the following approach was applied. It is known what is the form of the optimal Bell operator for the maximally entangled state $\rho_{ME} = |\psi_{ME}\rangle\langle\psi_{ME}|$, $|\psi_{ME}\rangle = \frac{1}{\sqrt{3}}(|++\rangle + |00\rangle + |--\rangle)$. Let us denote this optimal Bell operator by $\mathcal{O}_{\text{Bell}}^{ME}$.

For $\kappa = 1$ the state $|\psi_{ZZ}^{\text{scalar}}\rangle(m_1, m_2, c)$ (31) reduces to

$$|\psi_{ZZ}^{\text{scalar}}\rangle_{\kappa=1} = \frac{1}{\sqrt{3}}(|+-\rangle - |00\rangle + |-+\rangle). \quad (\text{B5})$$

Applying to $|\psi_{ZZ}^{\text{scalar}}\rangle_{\kappa=1}$ the operator $O_A \otimes I$, where

$$O_A = \begin{pmatrix} 0 & 0 & 1 \\ 0 & -1 & 0 \\ 1 & 0 & 0 \end{pmatrix}, \quad (\text{B6})$$

we obtain the maximally entangled state $|\psi_{ME}\rangle$. Thus, the optimal Bell operator for the state $|\psi_{ZZ}^{\text{scalar}}\rangle_{\kappa=1}$ has the form

$$(O_A \otimes I)^\dagger \mathcal{O}_{\text{Bell}}^{ME} (O_A \otimes I). \quad (\text{B7})$$

Next, we have

$$(U_A \otimes U_B) \sum_{\lambda\sigma} \Omega_{\lambda\sigma} |\lambda, \sigma\rangle = \sum_{\lambda\sigma} \Omega'_{\lambda\sigma} |\lambda, \sigma\rangle, \quad (\text{B8})$$

where

$$\Omega' = U_A \Omega U_B^T. \quad (\text{B9})$$

For the maximally entangled state $\Omega^{ME} = \frac{1}{\sqrt{3}}I$, thus this state is invariant on the action $U \otimes U^*$. Therefore, the optimal Bell observable for the state $|\psi_{ZZ}^{\text{scalar}}\rangle_{\kappa=1}$, instead of the form (B7) can be written in an equivalent form

$$(U O_A \otimes U^*)^\dagger \mathcal{O}_{\text{Bell}}^{ME} (U O_A \otimes U^*), \quad (\text{B10})$$

where U is an arbitrary unitary matrix. The value of \mathcal{I}_3 with the Bell operator given in (B10) in the state $|\psi_{ZZ}^{\text{scalar}}\rangle_{\kappa=1}$ is the same for all unitary matrices U .

For $\kappa \neq 1$ the Bell operator (B7) is no longer an optimal one. Moreover, different choices of U in (B10) lead to different values of \mathcal{I}_3 in this case. Thus, one can look for an optimal choice taking the Bell operator in the form (B10) and optimizing over all U matrices. This can be simplified further by observing that the state $(O_A \otimes I)|\psi_{ZZ}^{\text{scalar}}\rangle(m_1, m_2, c)$, according to (30, B9) is represented by the matrix

$$\Omega_{O_A} = \frac{1}{\sqrt{2 + \kappa^2}} \begin{pmatrix} 1 & 0 & 0 \\ 0 & \kappa & 0 \\ 0 & 0 & 1 \end{pmatrix}, \quad (\text{B11})$$

and that Ω_{O_A} is invariant under transformations (B9) with

$$U_A = \begin{pmatrix} \alpha & 0 & \beta \\ 0 & e^{i\phi} & 0 \\ \gamma & 0 & \delta \end{pmatrix}, \quad U_B = U_A^*, \quad \begin{pmatrix} \alpha & \beta \\ \gamma & \delta \end{pmatrix} \in SU(2). \quad (\text{B12})$$

Therefore, optimization can be restricted to U representing distinct cosets of $U(3)/(SU(2) \times U(1))$. In this paper, for the purpose of optimization, we used the following parametrization of U

$$U = \exp(i\Theta), \quad (\text{B13})$$

with

$$\Theta = \begin{pmatrix} 0 & e^{i\phi_1} R \cos \theta & 0 \\ e^{-i\phi_1} R \cos \theta & 0 & e^{i\phi_2} R \sin \theta \\ 0 & e^{-i\phi_2} R \sin \theta & 0 \end{pmatrix}. \quad (\text{B14})$$

To obtain Fig. 1, for each value of c we performed the optimization using the above parametrization. The optimal choice of R , θ , ϕ_1 , and ϕ_2 depends on the value of c , this change of parametrization is responsible for the cusp appearing in the plot.

2. Strategy 2

In this case we define a matrix

$$U_V(t) = \begin{pmatrix} \cos \frac{t}{2} & 0 & \sin \frac{t}{2} \\ 0 & 1 & 0 \\ -\sin \frac{t}{2} & 0 & \cos \frac{t}{2} \end{pmatrix} \quad (\text{B15})$$

and assume that observables used by Alice and Bob are represented by the following unitary matrices:

$$U_{A_1} = U_V(0), \quad U_{A_2} = U_V\left(\frac{\pi}{2}\right), \quad (\text{B16})$$

$$U_{B_1} = U_V(t), \quad U_{B_2} = U_V(-t). \quad (\text{B17})$$

Next, we are looking for such value of t which gives the highest violation of the CGLMP inequality. It appears that the optimal value is $t = -\frac{\pi}{4}$. We used this value to plot Fig. 1.

- [1] S. J. Freedman and J. F. Clauser, Experimental test of local hidden-variable theories, *Phys. Rev. Lett.* **28**, 938 (1972).
- [2] A. Aspect, J. Dalibard, and G. Roger, Experimental test of Bell's inequalities using time-varying analyzers, *Phys. Rev. Lett.* **49**, 1804 (1982).
- [3] M. Giustina, M. A. M. Versteegh, S. Wengerowsky, J. Handsteiner, A. Hochrainer, K. Phelan, *et al.*, Significant-loophole-free test of Bell's theorem with entangled photons, *Phys. Rev. Lett.* **115**, 250401 (2015).
- [4] M. A. Rowe, D. Kielpinski, V. Meyer, C. A. Sackett, W. M. Itano, C. Monroe, and D. J. Wineland, Experimental violation of a Bell's inequality with efficient detection, *Nature* **409**, 791 (2001).
- [5] B. Hensen, H. Bernien, A. E. Dréau, A. Reiserer, N. Kalb, M. S. Blok, *et al.*, Loophole-free Bell inequality violation using electron spins separated by 1.3 kilometres, *Nature* **526**, 682 (2015).
- [6] M. Ansmann, H. Wang, R. C. Bialczak, M. Hofheinz, E. Lucero, M. Neeley, *et al.*, Violation of Bell's inequality in Josephson phase qubits, *Nature* **461**, 504 (2009).
- [7] W. Pfaff, T. H. Taminiau, L. Robledo, H. Bernien, M. Markham, D. J. Twitchen, and R. Hanson, Demonstration of entanglement-by-measurement of solid-state qubits, *Nature Physics* **9**, 29 (2013).
- [8] A. Sinha and A. Zahed, Bell inequalities in 2-2 scattering, *Phys. Rev. D* **108**, 025015 (2023).
- [9] R. A. Morales, Exploring Bell inequalities and quantum entanglement in vector boson scattering (2023), arXiv:2306.17247 [hep-ph], arXiv:2306.17247 [hep-ph].
- [10] Y. Afik and J. de Nova, Entanglement and quantum tomography with top quarks at the LHC, *Euro. Phys. J. Plus* **136**, 907 (2021).
- [11] M. Fabbrichesi, R. Floreanini, and G. Panizzo, Testing Bell inequalities at the LHC with top-quark pairs, *Phys. Rev. Lett.* **127**, 161801 (2021).
- [12] J. A. Aguilar-Saavedra and J. A. Casa, Improved tests of entanglement and Bell inequalities with LHC tops, *Eur. Phys. J. C* **82**, 666 (2022).
- [13] R. Aoude, E. Madge, F. Maltoni, and L. Mantani, Quantum SMEFT tomography: Top quark pair production at the LHC, *Phys. Rev. D* **106**, 055007 (2022).
- [14] J. A. Aguilar-Saavedra, Post-decay quantum entanglement in top pair production (2023), arXiv: 2307.06991 [hep-ph], arXiv:2307.06991 [hep-ph].
- [15] Z. Dong, D. Gonçalves, K. Kong, and A. Navarro, When the machine chimes the Bell: Entanglement and Bell inequalities with boosted $t\bar{t}$ (2023), arXiv: 2305.07075 [hep-ph], arXiv:2305.07075 [hep-ph].
- [16] Y. Takubo, T. Ichikawa, S. Higashino, Y. Mori, K. Nagano, and I. Tsutsui, Feasibility of bell inequality violation at the atlas experiment with flavor entanglement of $B^0\bar{B}^0$ pairs from pp collisions, *Phys. Rev. D* **104**, 056004 (2021).
- [17] A. J. Barr, Testing Bell inequalities in Higgs boson decays, *Phys. Lett. B* **825**, 136866 (2022).
- [18] A. Barr, P. Caban, and J. Rembieliński, Bell-type inequalities for systems of relativistic vector bosons, *Quantum* **7**, 1070 (2023).
- [19] J. A. Aguilar-Saavedra, A. Bernal, J. A. Casas, and J. M. Moreno, Testing entanglement and Bell inequalities in $H \rightarrow ZZ$, *Phys. Rev. D* **107**, 016012 (2023).
- [20] R. Ashby-Pickering, A. J. Barr, and A. Wierzychucka, Quantum state tomography, entanglement detection and Bell violation prospects in weak decays of massive particles, *J. High Energy Phys.* **2023**, 20 (2023).
- [21] J. A. Aguilar-Saavedra, Laboratory-frame tests of quantum entanglement in $H \rightarrow WW$, *Phys. Rev. D* **107**, 076016 (2023).
- [22] M. Fabbrichesi, R. Floreanini, E. Gabrielli, and L. Marzola, Bell inequalities and quantum entanglement in weak gauge bosons production at the LHC and future colliders, *Eur. Phys. J. C* **83**, 823 (2023).
- [23] P. Caban, Helicity correlations of vector bosons, *Phys. Rev. A* **77**, 062101 (2008).
- [24] P. Caban, J. Rembieliński, and M. Włodarczyk, Einstein-Podolsky-Rosen correlations of vector bosons, *Phys. Rev. A* **77**, 012103 (2008).
- [25] A. M. Sirunyan *et al.* (CMS Collaboration), Measurements of the higgs boson width and anomalous $h\nu\nu$ couplings from on-shell and off-shell production in the four-lepton final state, *Phys. Rev. D* **99**, 112003 (2019).
- [26] M. Fabbrichesi, R. Floreanini, E. Gabrielli, and L. Marzola, Stringent bounds on HWW and HZZ anomalous couplings with quantum tomography at the LHC (2023), arXiv: 2304.02403 [hep-ph], arXiv: 2304.02403 [hep-ph].
- [27] R. Aoude, E. Madge, F. Maltoni, and L. Mantani, Probing new physics through entanglement in diboson production (2023), arXiv: 2307.09675 [hep-ph], arXiv:2307.09675 [hep-ph].
- [28] R. M. Godbole, D. J. Miller, and M. M. Mühlleitner, Aspects of CP violation in the HZZ coupling at the LHC, *J. High Energy Phys.* **2007**, 031 (2007).
- [29] T. Zagoskin and A. Korchin, Decays of a neutral particle with zero spin and arbitrary CP parity into two off-mass-shell Z bosons, *J. Exp. Theor. Phys.* **122**, 663 (2016).
- [30] Here, for convenience, we use vectors which are rescaled with respect to the basis vectors used in [24] or [18]. To obtain vectors used here one have to multiply those from [18] by $(2\delta^3(\mathbf{0})\sqrt{\omega_1\omega_2})^{-1}$.
- [31] R. L. Workman *et al.* (Particle Data Group), Review of Particle Physics, *PTEP* **2022**, 083C01 (2022).
- [32] H. E. Logan, Lectures on perturbative unitarity and decoupling in Higgs physics (2022), arXiv:2207.01064 [hep-ph], arXiv:2207.01064 [hep-ph].
- [33] M. Dahiya, S. Dutta, and R. Islam, Investigating perturbative unitarity in the presence of anomalous couplings, *Phys. Rev. D* **93**, 055013 (2016).
- [34] R. Rahaman and R. K. Singh, Breaking down the entire spectrum of spin correlations of a pair of particles involving fermions and gauge bosons, *Nucl. Phys. B* **984**, 115984 (2022).
- [35] Zagoskin and Korchin in [29] work in the helicity basis. Note that with our choice of the reference frame the sign of the third component of the spin for one of the bosons coincides with the helicity while for the other one with minus the helicity.
- [36] N. Brunner, D. Cavalcanti, S. Pironio, V. Scarani, and S. Wehner, Bell nonlocality, *Rev. Mod. Phys.* **86**, 419 (2014).
- [37] J. F. Clauser, M. A. Horne, A. Shimony, and R. A. Holt, Proposed experiment to test local hidden-variable theo-

- ries, Phys. Rev. Lett. **23**, 880 (1969).
- [38] D. Collins, N. Gisin, N. Linden, S. Massar, and S. Popescu, Bell inequalities for arbitrarily high-dimensional systems, Phys. Rev. Lett. **88**, 040404 (2002).
- [39] D. Kaszlikowski, L. C. Kwek, J.-L. Chen, M. Żukowski, and C. H. Oh, Clauser-horne inequality for three-state systems, Phys. Rev. A **65**, 032118 (2002).
- [40] S. Popescu and D. Rohrlich, Generic quantum nonlocality, Phys. Lett. A **166**, 293 (1992).
- [41] G. Vidal and R. F. Werner, Computable measure of entanglement, Phys. Rev. A **65**, 032314 (2002).
- [42] M. B. Plenio, Logarithmic negativity: A full entanglement monotone that is not convex, Phys. Rev. Lett. **95**, 090503 (2005).
- [43] A. Acín, T. Durt, N. Gisin, and J. I. Latorre, Quantum nonlocality in two three-level systems, Phys. Rev. A **65**, 052325 (2002).
- [44] A. Bernal, Quantum tomography of helicity states for general scattering processes (2023), arXiv: 2310.10838 [hep-ph], arXiv:2310.10838 [hep-ph].
- [45] A. Sirunyan *et al.* (CMS Collaboration), Measurements of production cross sections of the Higgs boson in the four-lepton final state in proton–proton collisions at $\sqrt{s} = 13$ TeV, Eur. Phys. J. C **81**, 488 (2021).
- [46] K. Rao, S. D. Rindani, and P. Sarmah, Study of anomalous gauge-Higgs couplings using Z boson polarization at LHC, Nucl. Phys. B **964**, 115317 (2021).